# Some Performance Characteristics of Spray Columns

S. VEDAIYAN, T. E. DEGALEESAN, G. S. LADDHA, and H. E. HOELSCHER

Chemical Engineering Department
A. C. College of Technology, University of Madras, Madras-25, India

Experimental data on the drop size distribution obtained from multiple nozzles in a spray column are presented and analyzed. For nozzles having a diameter above the critical size, the distribution pattern change from near normal monomodal to bimodal and back again to monomodal but skewed toward the larger size fraction. There is no change in the observed maximum drop size in the distribution with flow rate except near the critical velocity region. Drop breakup mechanisms appear to be different from the above pattern for nozzles below a critical size.

A model is proposed for prediction of the complete range of drop sizes observed.

The performance of a spray-type, liquid-liquid extraction column is dependent on the characteristics of the dispersion. This paper reports results from experiments conducted in the jetting range of nozzle velocities; a photographic analysis immediately above the nozzle was used to obtain the data reported. A model is proposed to characterize the drop size distribution from jetting to disruption velocities, this range being important in the normal operation of spray columns.

Relatively few photographic studies of drop size distributions have been reported and the available data are thus meagre. A detailed literature survey is available in the thesis of one of the authors (*26*) but the following references are particularly noteworthy. Keith and Hixson (*11*) noted that the uniformity of drops is related to the jet length. They observed that drops produced in the varicose region showed a high degree of uniformity when the jet length is below the critical value. In the sinuous region a decrease in uniformity was observed with an increasingly wide range of drop sizes. They showed the variation of drop uniformity on a normal probability plot of number count and observed that drops formed are most uniform in size near the critical velocity through the nozzle corresponding to the maximum jet length. Hinze (*9*) studied the maximum stable drop size under shear or turbulent flow, as in a rotary annular column, and suggested that the penetration of lamellae and ligaments of one liquid into another causes disintegration. He suggests that when a long ligament breaks into droplets, secondary smaller droplets are usually formed. Moreover, the ligaments at the moment of breakup will generally not be equally thick and hence, during the distintegration process, drops of different sizes are formed. Christiansen and Hixson (*2*) stated that the growth of the axially symmetric disturbance causes jet disintegration and that flow rates above the critical velocity produce more nearly random drop distributions. Using high speed photographs of the jets they observed that, near the region of instability, a number of nodes exist along the jet profile. Any untimely separation of the nodes upstream produced a drop larger than the ideal one-wave-length drop. The simultaneous disruption of two or more nodes produced small and large drops from the same jet.

Weaver et al. (*27*) photographed drop swarms during the operation of a spray column and observed that the droplet distribution characteristics did not change noticeably along the length of the column. They showed that the normal probability plot of diameter against cumulative volume yielded straight lines indicating a Gaussian distribution. Further, with a variation of flow rates, uniform slopes were obtained indicating a constant variance of the distribution. Latan and Kehat (*15*) observed that, for conditions

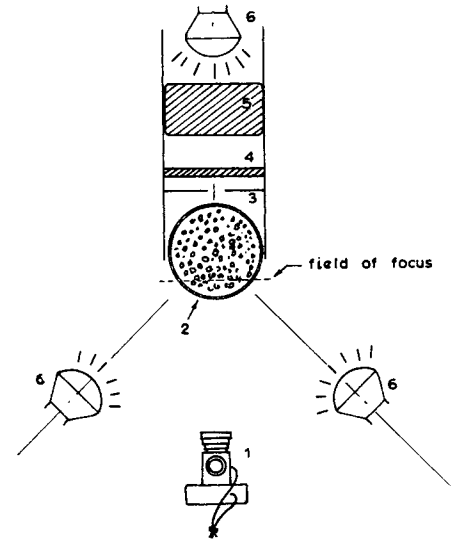


Fig. 1. Experimental photographic set up (plan view). 1. Leica M3 camera with visoflex attachment. 2. Spray column. 3. Light shield with aperture. 4. Frosted diffuser glass plate. 5. Filter solution. 6. Bright light sources.

Correspondence concerning this article should be addressed to H. E. Hoelscher at the School of Engineering, University of Pittsburgh, Pittsburgh, Pennsylvania 15213.

below flooding, the plots of drop sizes against the corresponding volume fraction equal to or smaller than that size on probability paper gave parallel straight lines as observed by Weaver et al. The median drop size was used to represent the average drop size of the distribution.

Although the drop size distribution is known to be important, particularly in the evaluation of the interfacial area, little is known about the actual size range of droplets in the distribution. Even the few investigations reported for spray columns do not present useful drop size distribution data. This paper presents a complete analysis of drop size distribution data obtained in a counter-current liquid-liquid spray column. The column was operated in the jetting range through a wide range of nozzle sizes. Analysis of drop sizes and their distribution were studied as a function of flow rate through the nozzles at specific continuous phase flow rates up to the flooding velocities.

## EXPERIMENTAL METHOD

The photographic study of drop sizes and their distribution was carried out in a 5 cm. I.D. spray column. The dispersion was produced by seven sets of distributor nozzles, varying in number and sizes, the complete characteristics of which are presented in Table 1.

The arrangement used for photographing the droplets is shown schematically in Figure 1. Details of the spray column experimental setup and the experimental procedure for column operation are the same as that adopted conventionally (Elgin

Table 1. Nozzle Characteristics

| Distributor No. | Nozzle diam., mm. | No. of nozzles | $a_T/a_n$ |
|---|---|---|---|
| A | 1.00 | 24 | 109.5 |
| B | 2.00 | 12 | 52.0 |
| C | 2.90 | 12 | 25.7 |
| D | 3.70 | 12 | 16.0 |
| E | 4.75 | 12 | 9.7 |
| F | 2.90 | 22 | 14.0 |
| O | 1.00 | 12 | 219.0 |

method) and have been described elsewhere (*26*). The simple photographic technique suggested by Damon et al. (*4*) was adopted with improved frontal lighting. An organic blue dye ("Cibacron Turquoise Blue G") at concentrations of 0.5% in water was used in the filter bath to provide blue rear light. This improved the contrast by sharply silhouetting the drops against a bright background and also absorbed the heat liberated by the rear lamp. Uniform illumination was provided by a light-diffusing frosted glass plate. The light shield with a circular aperture immediately behind the column eliminated all extraneous light except that which passed directly through the central region of the column.

Photographs of the drop swarms were obtained (when the column was operating under steady state condition) using a Leica M3 camera with visoflex attachment. Exposures of approximately 0.001 sec. were used. This produced sharp outlines at all flow rates. Photographs were taken through the glass wall of the column and the area photographed was about 18 mm. high and 22 mm. wide. The camera was focused onto a vertical

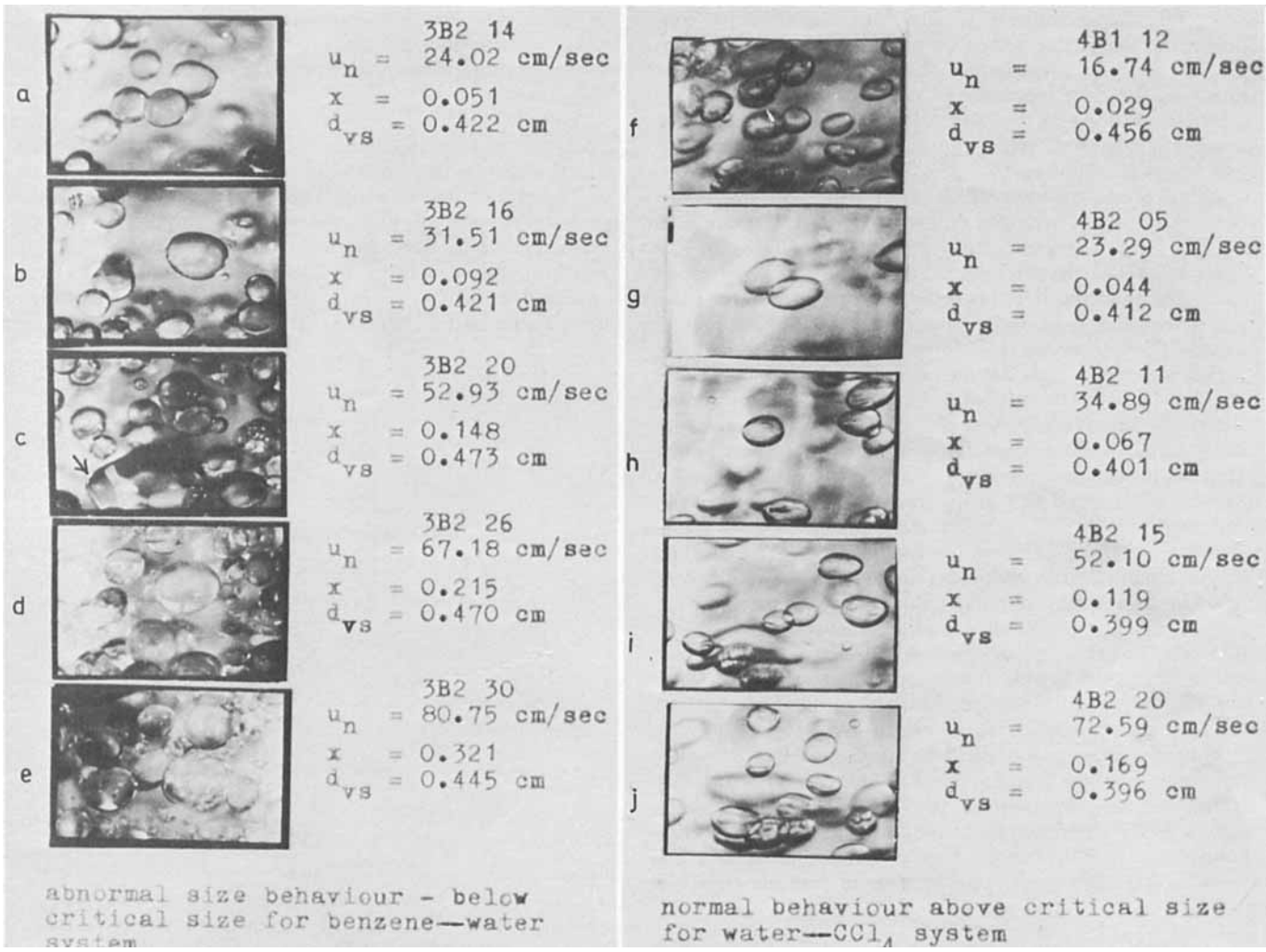


Fig. 2. Photographs of dispersions showing nozzle behavior for two typical systems, (nozzle diam. = 0.2 cm., number of nozzles 12, $u_c$ cm./sec. = 0).

TABLE 2. LIQUID CHARACTERISTICS

| S. No. | Continuous phase | Dispersed phase | $\rho_c$, g.-mole/cc. | $\rho_d$, g.-mole/cc. | $\mu_c$, cp | $\mu_d$, cp | $\gamma$, dynes/cm. | Refractive Index: Continuous phase | Refractive Index: Dispersed phase | Temp., °C. |
|---|---|---|---|---|---|---|---|---|---|---|
| 1. | Water | Methyl isobutyl ketone | 0.9917 | 0.7954 | 0.8494 | 0.6656 | 8.8 | 1.3340 | 1.3922 | 29 |
| 2. | Water | Isoamyl alcohol | 0.9906 | 0.8269 | 1.0090 | 2.7463 | 4.9 | 1.3363 | 1.3977 | 28 |
| 3. | Water | Benzene | 0.9956 | 0.8669 | 0.8554 | 0.6057 | 24.3 | 1.3322 | 1.4950 | 29 |
| 4. | Carbon tetrachloride | Water | 1.5826 | 0.9977 | 0.9484 | 0.8736 | 42.4 | 1.4545 | 1.3330 | 29 |

field at a distance 1.0 cm. away from the inner central axis of the column and the position of the camera was held fixed throughout the experiment. Usually 8 to 10 replicate photographs were taken at low flow rates and 6 to 8 at high flow rates. The photographed size of the droplets was 1½ times the actual size. Processed negatives were used directly for the measurements of drop sizes.

Sample photographs are shown on Figure 2.

The correction factors for the effect of refractive indices of field-liquid and column and for the curvature effect of the column were determined by standardizing with a glass bead of a known size inside the column at the field of focus with respect to the fixed position of the camera. To standardize, glass beads were chosen with sizes approximating the mean drop size encountered from visual observation of the drops. The details of the standardization procedure adopted in this study are described in Appendix A. Correction factors were applied to the measured horizontal and vertical diameters of the drops to translate the photographed image to true image. From the true lengths of major and minor axes, $d_1$ and $d_2$ respectively, the equivalent diameters of the corresponding spheroidal droplets were calculated. The number of drops measured for each flow rate varied from approximately 25 when the drops were of uniform size to approximately 100 when the drops varied in size considerably.

About 15,000 drops were measured in the photographic analysis of drop swarms covering various liquid-liquid systems. These are detailed in Table 2. A total of 600 ft. of 35 mm. film (Kodak Tri-X and ORWO NP-7) was used. Reproducibility of the data was carefully checked and found to be satisfactory. In all these cases, reproducibility was found to be well within the accuracy of the photographic calibration (*26*). Further comment on this appears in a later section. These films have been carefully preserved for future reference.

Technical grade solvents and laboratory distilled water were used after mutual saturation. All runs were taken at room temperature in the absence of transfer between phases.

### Size Distribution Analysis

Sample size frequency distributions of droplets as measured are shown by the solid lines on the histograms of Figure 3 for the isoamyl alcohol-water system. Isoamylalcohol was fed through a distributor. The flow through the nozzle varied from 9 to 88 cm./sec. It may be observed from these figures that, for low flow rates, the distribution remains normal or Gaussian with minimum deviation (curves A, B, and C). An increase in flow rate improves the distribution, showing more uniformity in drop size (curve C). At higher flow rates (curves E and F) the distribution becomes bimodal. At still higher flow rates the second of the two modes (curve D) increases in area while the first decreases and, at still higher flow rates, the bimodal curve again becomes monomodal but skewed toward larger drop sizes (curves G and H). Size frequency distribution curves prepared for other systems and nozzles showed that the distribution of drop sizes always varied from a near normal distribution (Gaussian) to bimodal and back again to monomodal with changing nozzle velocities for all systems studied. In the second monomodal stage the curves were highly skewed toward larger sizes as the flow rate was increased, thus showing the continuity in the changing pattern of size frequency distribution with flow rate. A typical integrated plot showing the "monomodal-bimodal-monomodal" behavior is represented in Figure 4.

Nozzle size had no effect on drop distribution pattern. Use of various diameters of nozzles for any specific system did not show any change in the observed distribution pattern with variation in flow rate. The pattern of distribution in all these cases followed the characteristic 1-2-1 mode behavior. However, the onset of bimodality occurred at lower nozzle velocities as the nozzle size increased. For example, the onset of bimodality for 1-mm. nozzle for isoamyl alcohol water system occurred at a nozzle velocity of 23 cm./sec., whereas for 2 mm. nozzle this was observed at about 10 cm./sec. Again, the complete data have been reported elsewhere (*26*). For the size frequency distribution reported in Figure 3, the 95% confidence limits of $d_{av}$ varied between $\pm$ 0.0086 to $\pm$ 0.0266 for the range of results from the most uniform size to a skewed distribution respectively. In percentage terms this corresponds to 3% to 18.5% through the same range of results.

The continuous phase flow rate in the range studied up to 0.75 cm./sec. was found to have negligible effect on the drop size distribution.

Henton and Cavers (*8*) recently reported a bimodal distribution for methyl isobutyl ketone water system using a nozzle diameter of 0.262 cm. The bimodality was reported by them at a flow rate of 10.97 cm./sec. through the nozzle. However, they did not make a detailed study covering a wide range of flow rates. Similar bimodal observations have been reported by Orr (*22*) for mineral spirit dispersed into water. In the case of solid grinding the 1-2-1 mode distribution of particle sizes has, of course, been frequently observed (*22*).

### Other Representations of Data

The data were also represented cumulatively on probability paper and on lognormal probability paper. These two distributions confirm observations noted in the previous section. The plots are noted to be nearly linear in the former case, but to show marked curvature in the lognormal distribution at low cumulative drop volume percentages. Previous observations (*27, 12*), that the variance is constant at all flow rates is in contrast with observations from this study and may be due to previous neglect of small droplets in the ensemble.

The suggestion of Yaron and Gal-Or (*28*) for a correlation using a dimensionless radius ratio against cumulative drop volume failed for this study; no single function was found adequate to represent the entire distribution. The ratio of Sauter-mean to volume-mean diameter varied from 1.009 to 1.344 in the present study, as opposed to the single value of 1.148 derived by Gal-Or and Hoelscher (*6*).

The upper limit distribution suggested by Mugele and Evans (*17*) failed at low flow rates though it successfully represented the distribution at high flow rates. The upper limit distribution function may be suitable only to predict a skewed distribution as in the present case at higher flow rates or the distribution obtainable in Rotary Disc Column illustrated by Olney (*21*).

### Uniformity Analysis

The solid line on Figure 5 records the variation in standard deviation of the experimental results with nozzle velocity to indicate the uniformity of the drop size distribution. Average drop diameter and standard deviation were calculated by techniques frequently recorded in the literature.

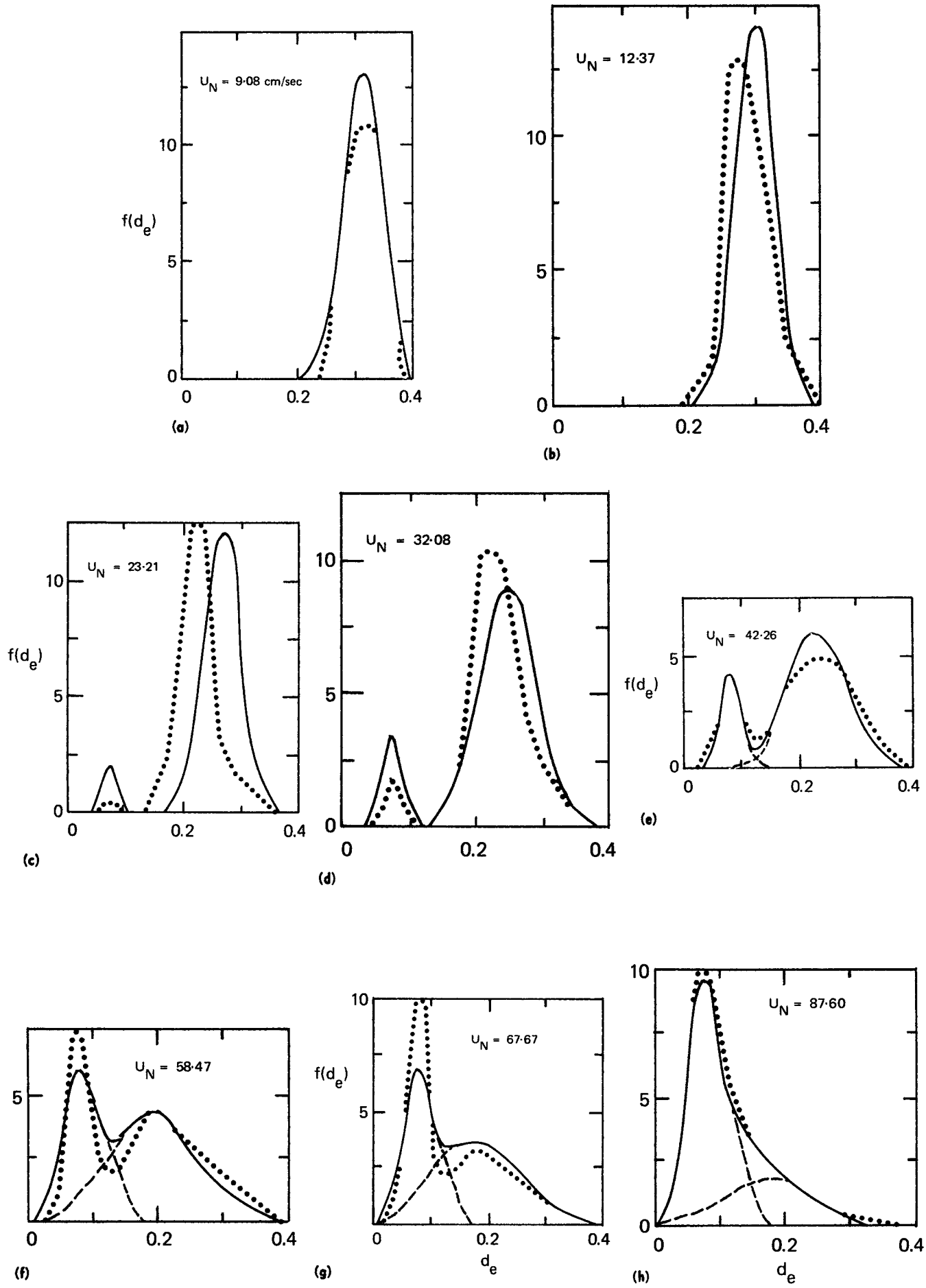


Fig. 3. Size frequency distribution —— Experimental data, – – – – – dissection for model, and ..... predicted results.

Two flow rate regions are again observed, the varicose and the sinuous, in agreement with previously recorded observations (*11, 1*). However, these results are different from those of Keith and Hixson whose data largely fall below a standard deviation of 0.04 but show the same general shape as a function of volume flow rate presented by the solid line on Figure 5. The relatively large values of standard deviation reported in this work could only occur as a result of the skewed drop size distribution observed. Studies of the residence time distribution of the dispersed phase using a dye technique confirm the variance characteristics of the distribution with progressive increases in nozzle velocity as shown on Figure 5 (*13*).

### Distribution of Rise Time of Drops

Visual observation of the column operation indicated that after their breakup from the jets drops in mutually saturated liquid phases did not coalesce during the rise period in the column. If this is so, the distribution of drop rise times observed in the column should give rise to the distribution of drop residence times.

The method of residence time analysis from drop size distribution was obtained using the function

$$F_n = \int_{t_{\min}}^{\infty} t^n f(x)\, dt \qquad (1)$$

After normalization, the mean and the variance of the distribution (the first and second moments respectively) were obtained by standard mathematical technique. The drop terminal velocities corresponding to each size fraction $f(x)$ were obtained from the correlation proposed by Krishnaswamy et al. (*14*). In each case the limits of integration being $t = t_{\min}$ (when $d_e = d_m$) to $t \rightarrow \infty$ (when $u_t \rightarrow 0$). $f(x)/F_0$ is given as a function of $t/\bar{t}$ in Figure 6.

It may be observed from this figure that there exists a drop rise time distribution which varies from a near normal one at low flow rates (plug flow) to a highly skewed distribution (back mixing) at high flow rates. Thus the dispersed phase velocity distribution must also show a similar trend related to drop size distribution.

### Critical Nozzle Size

The changeover from uniformity to nonuniformity in drop size distribution was marked by the appearance of smaller drops along with larger drops. Figure 2 also shows a typical sequence of photographs of drop ensembles at various flow rates employing two sets of nozzles. Also the distribution plots show that the largest drop encountered in the high flow rate regions is about the same size as that produced at low flow rates. However, for two systems (methyl isobutyl ketone-water and benzene-water), the use of nozzles of diameter below the critical value of $\frac{1}{2}(\gamma/\Delta\rho g)^{1/2}$ showed the sudden appearance of abnormally large-sized drops (indicated by arrow in Figure 2). Keith and Hixson (*11*) also noted the sudden appearance of larger drops in their experiments and observed that the constant increase in interfacial area with increase in flow rate ceased at this point.

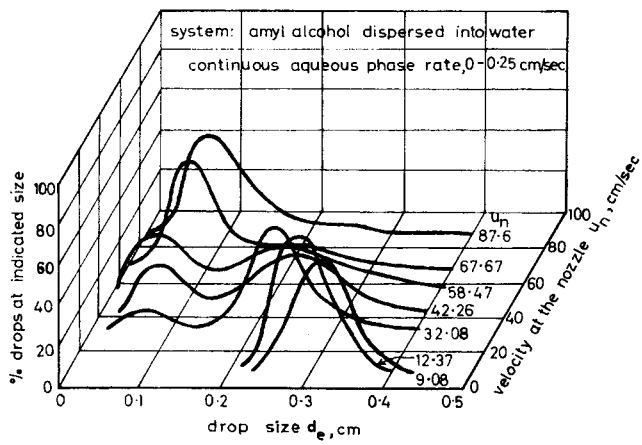


Fig. 4. Distribution of dispersed drops in a spray column.

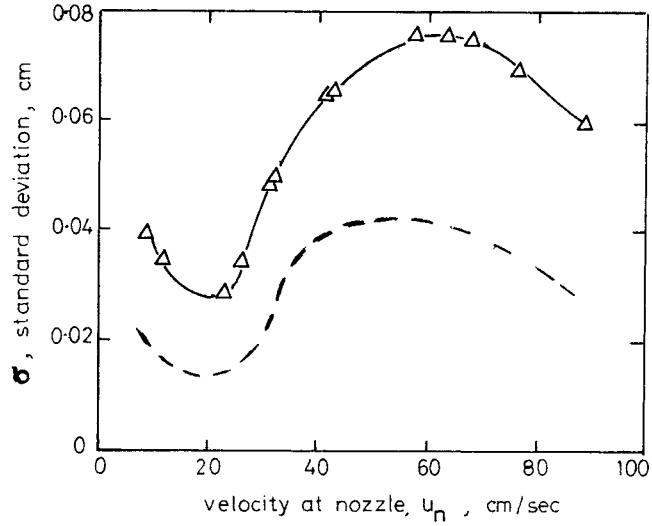


Fig. 5. Uniformity of drops.

## SUMMARY OF EXPERIMENTAL RESULTS

1. In the operation of a liquid-liquid spray column below flooding, drop size uniformity could be related to the two flow rate regions, namely, the varicose and the sinuous regions. In the varicose region as the flow rate through the nozzle is increased from jetting velocity to the critical velocity, the drop size uniformity increases. In the sinuous region the drop size nonuniformity increases as the flow rate through the nozzle is increased above the critical velocity.

2. The size frequency distribution, based on drop number count, showed a change from near normal monomodal to bimodal and back to monomodal as the flow rate through the distributor nozzle increased from jetting velocity to disruption velocity. This reproducible sequence of events, observed for a variety of liquid-liquid dispersions, is thought to be a new observation reported for the first time.

3. Analysis based on the volume fraction of drops indicated that the drop volume in each size fraction remained normally distributed at all flow rates.

4. The maximum size of droplets produced by the nozzles in the sinuous nonuniform region was nearly equal to the maximum size of droplet formed at the nozzle tip at very low flow rates.

5. The rise time distribution of droplets in the swarm as well as their velocity distribution indicated a change from a normal distribution to a skewed one as the flow rate of the dispersed phase was increased.

6. For nozzles of diameters greater than the value $\frac{1}{2}(\gamma/\Delta\rho g)^{1/2}$ the changeover from uniformity to nonuniformity was marked by the sudden appearance of large size droplets at periodic intervals. This phenomenon requires further investigation.

## PROPOSED MODEL

In spite of an increasing interest in distribution behavior of particles and droplets, part of the general field of particle technology, attempts to propose a proper distribution function to characterize even simple skewed distribution patterns are meagre. No successful method has thus far been reported for obtaining a mathematical function to describe the continuously changing pattern of size distri-

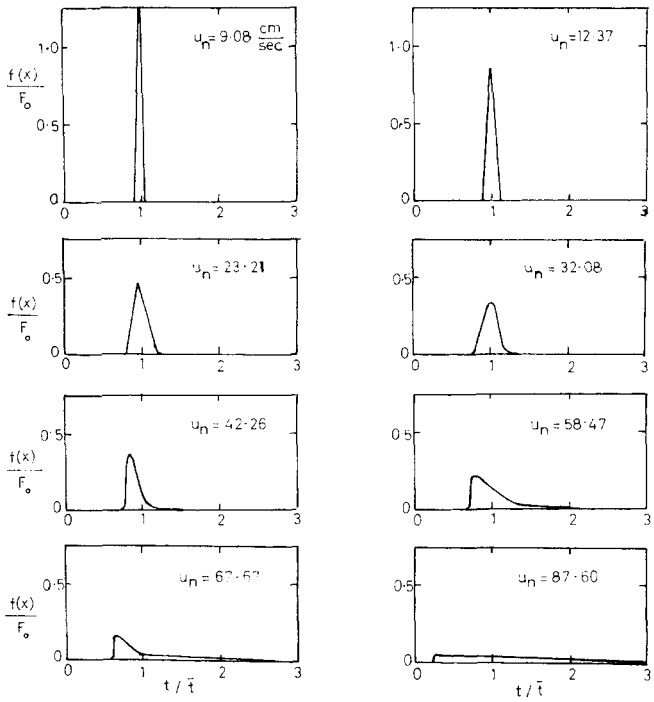


**Fig. 6. Drop rise time distribution.**

bution of particles, even for comminution of solids. Most of the statistical methods available in the literature are based on the distribution studies for normal, lognormal, skewed, upper limit distribution, etc. (*12, 17, 19, 24*). These equations are not obviously modifiable for description of a bimodal distribution, much less of a changing pattern. The only attempt that has been reported in the literature is that by Dallavalle et al. (3) for a bimodal size frequency distribution encountered in micromeritics. The proposed equation is an algebraic series in an exponential, a form which clearly cannot successfully predict the distributions observed from this work.

The method for modeling results obtained from this study is based in the observed characteristics of the drop size distributions, Figure 3. These are as follows: 1. In the bimodal region the second mode commences at the critical flow rate and increases gradually with the flow rate, then assuming prominence; however, the mean of the smaller size fraction is independent of flow rate; 2. The first mode which is high and narrow near the critical velocity becomes wider and lower with increase in the flow rate. The peak of this latter mode gradually shifts toward the smaller size fraction showing the dependency on flow rate.

The dashed lines on Figure 3 show the method of dissection used to split the bimodal distribution into two normal distributions. As the distribution is normalized, the total area under the two curves will be unity but the distribution of areas under the two curves will be a function of flow rate, since above the critical velocity the area corresponding to the lower fraction increases while the other decreases.

The proposed two normal distributions can then be written and the final equation for the distribution obtained by addition of the two number densities. This seems justified since the two distribution equations are derived from the same drop population. Setting $A$ and $(1 - A)$ to be the areas under the upper and lower size distribution curves, $\sigma_1$ and $\sigma_2$ the standard deviations of the two normal distributions and a dimensionless velocity equal to the ratio of any nozzle velocity to the critical nozzle velocity, we find two regions. Region 1 is that wherein the dimensionless velocity is less than unity and the distribution normal with the uniformity increasing as the dimensionless velocity approaches as one. In region 2, where the dimensionless velocity is greater than unity, the nonuniformity increases from the onset of bimodality where $u = 1$.

A single distribution function can then be written as follows

$$f(x, u) = \frac{1}{\sqrt{2\pi}} \left[ \frac{A}{\sigma_1} \exp\left( - \frac{(x - \bar{x}_1)^2}{2\sigma_1^2} \right) + \frac{1 - A}{\sigma_2} \exp\left( - \frac{(x - \bar{x}_2)^2}{2\sigma_2^2} \right) \right] \quad (2)$$

The data show that the mean of the lower size fraction remains constant at

$$\bar{x}_2 = 0.2 \quad (3)$$

from the onset of bimodality to disruption of the jet. Further, for the two normal distributions, when treated individually, the standard deviation of the lower size fraction varied, with the standard deviation of the upper size fraction bearing approximately a constant ratio given by

$$\frac{\sigma_1}{\sigma_2} = 3 \quad (4)$$

When $\sigma_2$ was replaced by $\sigma_1/3$ with mean $\bar{x}_2 = 0.2$ the distribution under the lower size fraction could be described without appreciable error. Substituting the values given in Equations (8) and (9) and replacing $\bar{x}_1$ by $\bar{x}$ and $\sigma_1$ by $\sigma$ Equation (2) can be written as

$$f(x, u) = \frac{A}{\sqrt{2\pi}\,\sigma} \left[ \exp\left( - \frac{(x - \bar{x})^2}{2\sigma^2} \right) + B \exp\left( - \frac{9(x - 0.2)^2}{2\sigma^2} \right) \right] \quad (5)$$

Defining the distribution parameter $\delta$ as

$$\delta = 2\sigma^2 \quad (6)$$

Equation (5) can be rewritten as

$$f(x, u) = \frac{A}{\sqrt{\pi\delta}} \exp\left( - \frac{(x - \bar{x})^2}{\delta} \right) + B \exp\left( - \frac{9(x - 0.2)^2}{\delta} \right) \quad (7)$$

where

$$B = 3(1 - A)/A \quad (8)$$

and $\bar{x}$ is the mean of the uppersize fraction.

The detailed analysis of the distribution for dependence of the three constants $\bar{x}$, $\delta$, and $A$ in Equation (7) on the independent variable gives the following three equations

$$\bar{x} = 0.88 \exp(-0.175\,u) \quad (9)$$

$$\delta = 0.04 + 0.03 \sin \pi \left( \frac{u - 2.25}{2.5} \right) \quad (10)$$

$$A = \exp[-0.125\,(u - 1)], \quad u > 1 \quad (11)$$

For flow rates below the critical velocity ($u < 1$), if $A$ is set equal to unity ($A = 1$) the second term in Equation (7) vanishes.

The dotted lines on Figure 2 show the distribution predicted by Equation (7). This theoretical result is based on a critical velocity of 23 cm./sec. for a 1-mm. diameter nozzle with isoamyl alcohol dispersed into water. This critical velocity agrees well with 22.1 cm./sec. reported

by Keith and Hixson (*11*) for a nozzle of 1.15 mm. diameter. The maximum drop size was taken as 0.385 cm. which was the average of the maximum drop size encountered at all flow rates except near the critical velocity region. On Figure 2, the predicted curve (solid line) may be compared with experimental curve (dotted line) to see the agreement and the applicability of Equation (7). Further comparisons are made in Figure 7*a* and 7*b* for the average diameter, $d_{av}$ defined as

$$d_{av} = d_{max} \frac{\int_0^1 x f(x,u)\, dx}{\int_0^1 f(x,u)\, dx} \tag{12}$$

and the Sauter mean defined as

$$d_{vs} = d_{max} \frac{\int_0^1 x^3 f(x,u)\, dx}{\int_0^1 x^2 f(x,u)\, dx} \tag{13}$$

using the experimental values. The dashed line on Figure 5 shows the standard deviation for the theoretical distribution and may be compared with experimental values, the solid line, and the data points.

For the proposed equation, analyses made on lognormal probability plots with cumulative volume fraction indicate that the maximum drop size is the same for flow rates below and above the critical velocity, whereas the maximum drop size reaches a minimum at critical velocity. Similar plots on normal probability paper showed the increasing tendency to uniformity toward the critical velocity and, thereafter, nonuniformity away from the critical velocity. Straight line plots in the normal probability graph indicate that the volume of smaller size fraction is small. This agreed with the observations of Weaver et al. (*27*) and Letan and Kehat (*16*). Although very little volume is occupied by this smaller size fraction as holdup in the column, as observed by Henton and Cavers (*8*), the area offered by these drops for mass transfer is considerable. In spite of the fact that the volume may remain normally distributed (when the smaller size fraction is neglected) the true distribution and the evaluation of the various means will result in higher values than the true means. Considering the data reported by Henton and Cavers (*8*) for methyl isobutyl ketone dispersion into water, the mean was taken as 0.342 cm., whereas the actual mean and Sauter mean were 0.189 cm. and 0.329 cm. when the whole distribution was taken into consideration. Accordingly, the specific area calculated will be in error by 10%.

The present approach offers a better procedure to evaluate the complete distribution for liquid-liquid dispersions. Only two parameters, namely, the maximum drop size and the critical velocity which are characteristic of nozzle diameter and liquid properties, need be known.

### Critical Velocity

Some correlations are available (*5, 10, 23*) to predict the critical velocity but they are not completely reliable for all nozzle ranges. Hughmark (*10*) from the analysis of Keith and Hixson's (*11*) data suggests that the critical velocity could be predicted by the equation

$$u_{nc} = 2.94 \sqrt{\frac{\gamma}{\rho_d\, d_n}} \tag{14}$$

Ranz (*23*) predicts that the nonuniform drop size begins at a critical velocity given by

$$u_{nc} = 2.83 \sqrt{\frac{\gamma}{\rho_c\, d_n}} \tag{15}$$

Though these two equations show fair agreement, the critical velocities predicted are too high for larger nozzles. However, these may be employed with fair accuracy in the range where $d_n$ varies from $\frac{1}{2}(\gamma/\Delta\rho g)^{1/2}$ to $(\gamma/\Delta\rho g)^{1/2}$.

### Maximum Drop Size

To predict the drop volume or drop diameters, the existing Equations (7), (18), (20), and (25) indicate a peak value with increase of flow rate through the nozzle in the region below jetting. The maximum drop size (that is the peak value) predicted by these equations may be used in the proposed model in the absence of any other correlation to predict the maximum drop size in the distribution.

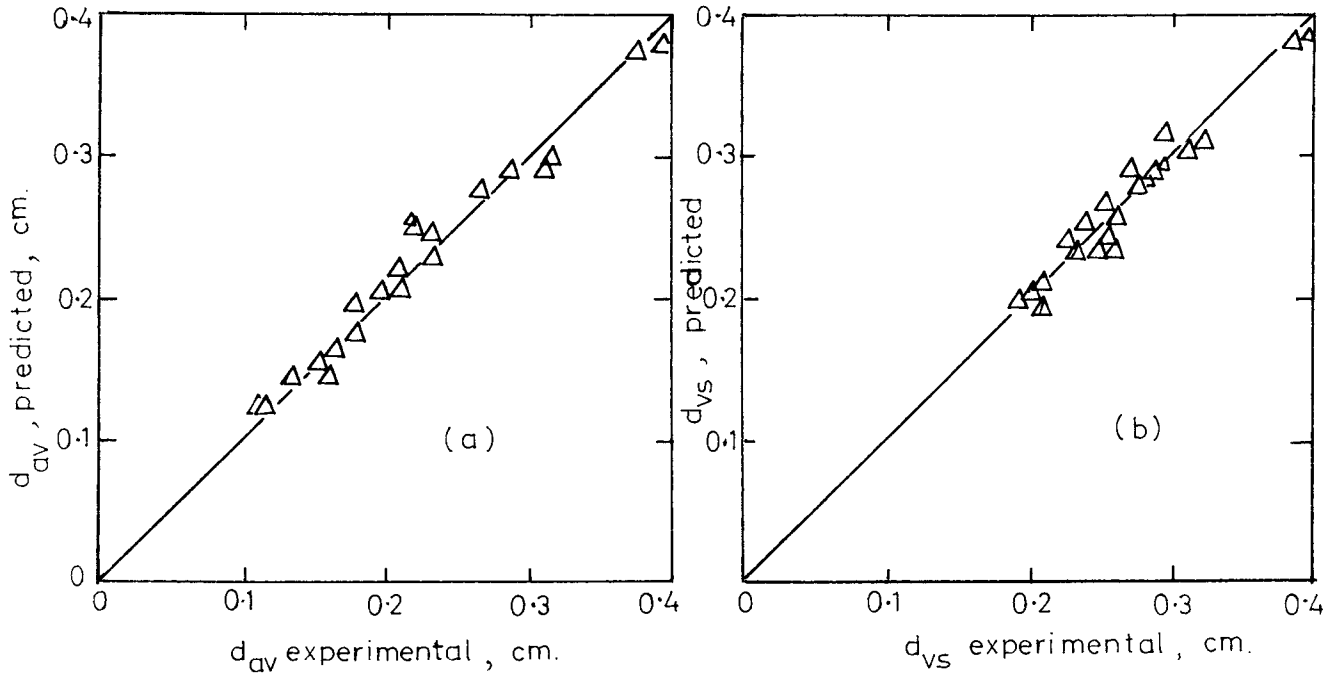


Fig. 7. Comparison of predicted and experimental diameters.

## SUMMARY FROM MODELING EFFORT

A mathematical model for the entire range of observed results is proposed. The model adequately describes the data from the mono- through the bi- and back to the monomodal distribution as a function of nozzle velocity and physical parameters of the system. The result permits estimation of the contribution to the transfer process from any segment of the drop population, in particular from the tails normally ignored when calculating transfer areas.

## NOTATION

$A$ = area under the normalized distribution curve
$B$ = constant defined by Equation (8)
$d_{av}$ = mean diameter of the distribution, cm., defined by Equation (12)
$d_e$ = equivalent diameter of sphere, having the same volume of spheroid with major and minor diameters $d_1$ and $d_2$, cm.
$d_{max}$ = maximum drop diameter in the ensemble, cm.
$d_n$ = nozzle diameter, cm.
$d_{vs}$ = volume-surface mean diameter, cm., defined by Equation (13)
$d_1$ = major diameter of spheroidal droplet, cm.
$d_2$ = minor diameter of spheroidal droplet, cm.
$F_n$ = $n$th moment
$F_0$ = zeroth moment
$f(x)$ = size frequency
$g$ = acceleration due to gravity, cm./sec.$^2$
$n$ = number of drops in each size fraction or the number of the moment—depending on context
$t$ = time, sec.
$\bar{t}$ = average residence time, sec.
$u$ = dimensionless velocity, $u_n/u_{nc}$
$u_n$ = mean velocity through the nozzles, cm./sec.
$u_{nc}$ = critical velocity at the nozzle, cm./sec.
$u_t$ = terminal velocity of drop, cm./sec.
$x$ = dimensionless diameter = $d_e/d_{max}$
$\bar{x}$ = mean of the normalized distribution

### Greek Letters

$\delta$ = distribution parameter, dimensionless
$\Delta\rho$ = density difference, g.-mole/cu.cm.
$\sigma$ = standard deviation, dimensionless
$\gamma$ = interfacial tension, dynes/cm.

### Subscripts

1 = distribution under larger size fraction
2 = distribution under smaller size fraction
min. = minimum

## LITERATURE CITED


1. Brodkey, R. S., "The Phenomena of Fluid Motions," p. 539, Addison-Wesley, Reading, Mass. (1967).
2. Christiansen, R. M., and A. N. Hixson, *Ind. Eng. Chem.*, **49**, 1017 (1957).
3. Dallavalle, J. M., C. Orr, Jr. and H. G. Blocker, *ibid.*, **43** (1951).
4. Damon, K. C., J. B. Angelo, and R. W. Park, *Chem. Eng. Sci.*, **21**, 813 (1966).
5. Fujinawa, K., T. Maruyama, and Y. Nakaike, *Kagaku Kikai*, **21**, 194 (1957).
6. Gal-Or, B., and H. E. Hoelscher, *AIChE J.*, **12**, 499 (1966).
7. Hayworth, C. B., and R. E. Treybal, *Ind. Eng. Chem.*, **42**, 1174 (1950).
8. Henton, J. E., and S. D. Cavers, *Ind. Eng. Chem. Fundamentals*, **9**, 384 (1970).
9. Hinze, J. O., *AIChE J.*, **1**, 289 (1955).
10. Hughmark, G. A., *Ind. Eng. Chem. Fundamentals*, **6**, 408 (1967).
11. Keith, F. W., and A. N. Hixon, *Ind. Eng. Chem.*, **47**, 258 (1955).
12. Kelleher, J., *Brit. Chem. Eng.*, **4**, 464 (1960).
13. Krishnan, T. R., M. Tech. thesis, Madras Univ., India (1969).
14. Krishnaswamy, T. R., S. Chandramouli, M. G. Subba Rao, and G. S. Laddha, *Indian Chem. Eng.*, **9**, 59 (1967).
15. Letan, R., and E. Kehat, *AIChE J.*, **13**, 443 (1967).
16. *Ibid.*, **14**, 398 (1968).
17. Mugele, R. A., and H. D. Evans, *Ind. Eng. Chem.*, **43**, 1317 (1951).
18. Narasinga, Rao E. V. L., R. Kumar, and N. R. Kuloor, *Chem. Eng. Sci.*, **21**, 867 (1966).
19. Nukiama, S., and Y. Tanasawa, *Trans. Soc. Mech. Eng.* (Japan), **4**, 86 (1938).
20. Null, H. R., and H. F. Johnson, *AIChE J.*, **4**, 273 (1958).
21. Olney, R. B., *ibid.*, **10**, 827 (1964).
22. Orr, C. Jr., "Particulate Technology", p. 110, Macmillan, New York (1966).
23. Ranz, W. E., *Can. J. Chem. Eng.*, **36**, 175 (1958).
24. Rosin, P., and J. Rammler, *Inst. Fuel*, **7**, 29 (1933).
25. Scheele, G. F., and B. J. Meister, *AIChE J.*, **14**, 9 (1968).
26. Vedaiyan, S., Ph.D. thesis, Madras Univ., India (1969).
27. Weaver, R. E. C., L. Lapidus, and J. E. Elgin, *AIChE J.*, **5**, 533 (1959).
28. Yaron, I., and B. Gal-Or, *Intern. J. Heat Mass Transfer*, to be published.


## APPENDIX A. ASSESSMENT OF DROP DISTORTION IN THE COLUMN

The method of obtaining the correction factor for the horizontal and vertical axes of the drops is indicated schematically in Table A1. The actual area of the column under focus was 24 mm. × 16 mm. The glass bead of known dimensions was placed in various positions as indicated by the rectangles and photographed. From the developed negative films, the correction factors were obtained, by measuring the horizontal and vertical diameters and comparing with the true diameters. The correction factors as well as the measured horizontal and vertical diameters from the photographs are indicated in the corresponding rectangles. This method of obtaining the correction factors was carried out for each system after mutually saturating the systems and before taking experimental runs.

The readings in the table refer to the system where water was dispersed into carbon tetrachloride. From Table A1, it may be seen that the correction factor does not vary much with location inside the column and therefore average values of 1.540 for the horizontal diameters and 1.437 for the vertical diameters were taken.

Table A1. Measured Diameters and the Corresponding Correction Factors

Dimensions of glass bead
$D_H = 4.96$ $D_V = 5.04$

| | | |
|---|---|---|
| $D_H = 7.54$<br>$D_V = 7.22$<br>$C_1 = 1.520$<br>$C_2 = 1.433$ | $D_H = 7.56$<br>$D_V = 7.14$<br>$C_1 = 1.524$<br>$C_2 = 1.417$ | $D_H = 7.56$<br>$D_V = 7.12$<br>$C_1 = 1.524$<br>$C_2 = 1.415$ |
| $D_H = 7.67$<br>$D_V = 7.34$<br>$C_1 = 1.545$<br>$C_2 = 1.456$ | $D_H = 7.58$<br>$D_V = 7.36$<br>$C_1 = 1.528$<br>$C_2 = 1.460$ | $D_H = 7.66$<br>$D_V = 7.32$<br>$C_1 = 1.544$<br>$C_2 = 1.452$ |
| $D_H = 7.86$<br>$D_V = 7.30$<br>$C_1 = 1.585$<br>$C_2 = 1.448$ | $D_H = 7.82$<br>$D_V = 7.20$<br>$C_1 = 1.577$<br>$C_2 = 1.429$ | $D_H = 7.84$<br>$D_V = 7.28$<br>$C_1 = 1.577$<br>$C_2 = 1.445$ |

$D_H$, $D_V$—Horizontal and vertical measured diameters of bead.
$C_1$, $C_2$—Correction factors for horizontal and vertical diameters.

*Manuscript received April 27, 1971; revision received August 9, 1971; paper accepted August 16, 1971.*